ELSEVIER

Catalysis Today 67 (2001) 281–291

CATALYSIS TODAY

www.elsevier.com/locate/cattod

A study on the performance of a dense polymeric catalytic membrane reactor

José M. Sousa [a], Paulo Cruz [b], Adélio Mendes [b,*]

[a] *Chemistry Section, University of Trás-os-Montes e Alto Douro, Apartado 202, 5001-911 Vila-Real Codex, Portugal*
[b] *Chemical Engineering Department, LEPAE, Faculty of Engineering, University of Porto, Rua Roberto Frias, 4200-465 Porto, Portugal*

Abstract

A theoretical study on a catalytic polymeric dense membrane reactor (CPDMR) is performed. The conversion enhancement over the thermodynamic equilibrium value is studied for an equilibrium gas-phase reaction of the type $a\mathrm{A} + b\mathrm{B} \Leftrightarrow c\mathrm{C} + d\mathrm{D}$ for three different conditions: $\Delta n > 0$, $\Delta n = 0$ and $\Delta n < 0$, where $\Delta n = (c + d) - (a + b)$. For each of these cases, it is studied the influence of the reaction product sorption and diffusion coefficients. The model used considers perfectly mixed flow patterns and isothermal operation in the retentate and permeate sides. It is concluded that the conversion of a reversible reaction can be significantly enhanced when the diffusion coefficients of the products are higher than the reactants' and/or the sorption coefficients are lower. The extension of this enhancement depends on the reaction stoichiometry, global concentration inside the membrane, Thiele modulus and contact time values. It was also observed that it would be preferable to have a conversion enhancement based on higher product diffusion than on lower product sorption coefficients, since this leads to smaller reactor size. Since the performance of a dense membrane reactor depends on both the sorption and diffusion coefficients in a different way, a study of such a system cannot be based only on the permeabilities of the reaction components.

Keywords: Polymeric catalytic membrane reactor; Dense membrane; Gas-phase reactions; Equilibrium reaction; Modelling

1. Introduction

The energy efficiency and simplicity of membrane systems has been made growing them very attractive for separation processes. This technology has found a wide range of applications in gas separation and has become a standard operating unit for several applications [1]. Most of the commercially available membranes for gas separation are polymeric. Among other reasons, we can refer to the higher production complexity (control of the membrane thickness, large scale preparation, defects free) and cost of ceramic membranes [2–4]. Besides, polymeric membranes are not as brittle as the ceramic ones and can be easily fabricated in a number of forms (flat, tubes, tubules, hollow fibres, spiral wound) [1,5,6].

As the research on membrane separation technology developed, several authors started studying the integration of membranes in chemical reactors, performing different functions [5]. The early research in membrane reactors employed primarily polymeric membranes and enzymatic reactions. However, soon several petrochemical relevant reactions, where the membranes could become a key factor in obtaining a competitive process, were identified and interested several researchers. Dehydrogenations are one of the

---

[*] Corresponding author. Tel.: +351-22-5081695;
fax: +351-22-5081449.
E-mail address: mendes@fe.up.pt (A. Mendes).

PII: S0920-5861(01)00315-7

Nomenclature

a, b	stoichiometric coefficient for the reactants (–)
c, d	stoichiometric coefficient for the reaction products (–)
C_{ref}	reference concentration (mol/m^3)
D_i	diffusion coefficient of component i (m^2/s)
D_{ref}	reference diffusion coefficient (m^2/s)
H_i	Henry's sorption coefficient of component i (mol/(m^3 Pa))
H_{ref}	reference Henry's sorption coefficient (mol/(m^3 Pa))
k_{d}	direct reaction rate constant (m^3/(mol s))
K_{e}	reaction equilibrium constant ((mol/m^3)$^{\Delta n}$)
L_i	permeability of component i (mol m/(s m^2 Pa))
L_{ref}	relative permeability (mol m/(s m^2 Pa))
Δn	total net change of the number moles (–)
p_i	partial pressure in equilibrium with the concentration of component i inside the membrane (Pa)
p_i^{F}	partial pressure of component i in the feed (Pa)
p_i^{P}	partial pressure of component i in the effluent permeate (Pa)
p_i^{R}	partial pressure of component i in the effluent retentate (Pa)
P_{ref}	reference pressure (Pa)
P^{P}	total pressure in the permeate side (Pa)
P^{R}	total pressure in the retentate side (Pa)
Q_{ref}	reference volumetric flowrate (m^3/s)
Q^{F}	total feed volumetric flowrate (m^3/s)
Q^{P}	total permeate volumetric flowrate (m^3/s)
Q^{R}	total retentate volumetric flowrate (m^3/s)
$\mathfrak{R}$	ideal gas constant (Pa m^3/(mol K))
S	membrane surface area (m^2)
T	absolute temperature (K)
TPL	total permeation line (–)
x	dimensionless membrane spatial coordinate (–)
X_{A}	conversion of reactant A (–)
$X_{\mathrm{A}}^{\mathrm{e}}$	thermodynamic equilibrium conversion of reactant A based on feed conditions
z	membrane spatial coordinate (m)

Greek symbols

α_i	dimensionless diffusion coefficient of component i (–)
β	direct reaction order (–)
γ_i	dimensionless sorption coefficient of component i (–)
Γ	dimensionless contact time (–)
δ	membrane thickness (m)
ζ^{P}	dimensionless total permeate volumetric flowrate (–)
ζ^{R}	dimensionless total retentate volumetric flowrate (–)
θ	reaction coefficient ((mol/m^3)$^{\Delta n}$)
λ_i	dimensionless permeability of component i (–)
ν_i	stoichiometric coefficient of component i (–)
ρ	dimensionless local reaction rate (–)
Φ	Thiele modulus (–)
χ_{A}	relative conversion (ratio between X_{A} and $X_{\mathrm{A}}^{\mathrm{e}}$) (–)
Ψ_i	dimensionless partial pressure in equilibrium with the concentration of component i inside the membrane (–)
Ψ^{P}	dimensionless total pressure in the permeate (–)
Ψ^{R}	dimensionless total pressure in the retentate (–)
Ψ_i^{F}	dimensionless partial pressure of component i in the feed (–)
Ψ_i^{P}	dimensionless partial pressure of component i in the effluent permeate (–)
Ψ_i^{R}	dimensionless partial pressure of component i in the effluent retentate (–)

such class of reactions with considerable practical importance, because many commodity chemicals (for example ethylene, propylene, butenes and styrene) are produced by catalytic cracking of low molecular weight hydrocarbons [7]. These reactions are endothermic and equilibrium limited and to attain reasonable conversions, it is necessary to carry out the reaction at high temperature (typically 750–950°C [8]). However, high operating temperatures results in high energetic costs and catalyst deactivation. One way to lower the temperature of these reactions and maintaining the yield is to conduct the process in a membrane reactor. This strategy has been extensively studied for alkane dehydrogenation with different kind of membranes, namely metallic (palladium or palladium alloys) [9–12], ceramic [13–16], composite [17–19] and carbon membranes [20]. For these applications, the reactor normally used is the so-called packed bed membrane reactor (PBMR), where the membrane only performs a selective removal of hydrogen.

Due to the high temperatures and, in some cases, the aggressive chemical environments, it is not surprising that polymeric catalytic membranes were hardly ever used, as they lack thermal and chemical stability under these harsh conditions. So, polymeric catalytic membrane reactors must find their own opportunities of application in systems with much milder thermal and chemical conditions, even considering that the commonly used polydimethilsyloxane (PDMS) is thermally stable up to 523 K [2] and that there are some promising ways of creating polymeric materials with significant chemical and thermal resistance [21].

The research on polymeric catalytic materials has been focused mainly in liquid phase reactions under mild conditions, namely in fine chemical synthesis [6,22–28]. The selectivities in gas phase are normally lower than in liquid phase, but on the other hand, the reaction can be conducted in a solvent free medium, avoiding a further separation process to remove it. However, the research in gas-phase reaction with polymeric catalytic membranes is still limited [8,29–35], being the selective hydrogenations the most important set of reactions referred up to now [29,32–34]. Also, polymeric catalytic membranes can be used to enhance the conversion over the thermodynamic equilibrium, for equilibrium limited reactions [23,36].

Several studies focusing on modelling membrane reactors with [28,37–40] or without [41–48] coupled experimental work, can be found in the open literature. However, most of these studies deal with PBMR and only a few actually focus on catalytic membrane reactors, CMR (where the catalyst is either the membrane itself, or it is incorporated in the porous membrane structure, or on the membrane surface, or it is occluded inside the membrane) [28,37,38,40,42,44,46]. At the best of our knowledge, in addition to our recent work [42], only Kaliaguine and co-workers [28] modelled a catalytic dense polymeric membrane reactor, but for conducting a liquid phase reaction.

In the present paper, a systematic theoretical study is performed, focusing mainly on how the CPDMR conversion for an equilibrium gas-phase reaction is affected by the reaction stoichiometry, for a set of selected cases of reaction product diffusion and sorption coefficients.

2. Model development

The catalytic polymeric dense membrane reactor (CPDMR) considered in the present study is sketched in Fig. 1. It consists of a retentate and permeate chambers at different total pressures P^{R} and P^{P}, respectively, separated by a catalytic membrane of thickness δ and with the catalyst homogeneously distributed throughout it.

A hypothetical gas-phase reaction of type $a\mathrm{A} + b\mathrm{B} \Leftrightarrow c\mathrm{C} + d\mathrm{D}$ is considered and three different cases are studied: $\Delta n > 0$, $\Delta n = 0$ and $\Delta n < 0$, where $\Delta n = (c+d) - (a+b)$. The model developed is based on the following main assumptions [42]:

1. Steady-state operation.
2. Isothermal operation.
3. Perfectly mixed flow pattern on both retentate and permeate chambers.
4. Negligible total pressure drop in the retentate and permeate chambers.
5. Negligible external transport limitations in the membrane/gas-phase interfaces.
6. Fickian transport across the membrane.
7. Constant diffusion coefficients.

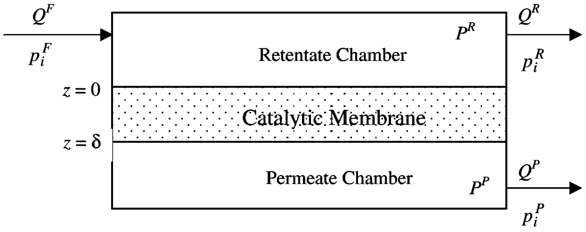

Fig. 1. Schematic diagram of the CPDMR.

8. Linear sorption equilibrium isotherm between the bulk gas phase and the membrane surface.
9. Elementary reaction mechanism referred to a membrane volume.
10. The reaction occurs only on the catalyst nanoparticles surface.
11. Equal concentration in the catalyst surface and polymer.

The mathematical model comprises steady-state mass balances for the membrane, retentate and permeate chambers, with the respective boundary conditions. The dimensionless form of the model equations is as it follows [42]:

Mass balance in the membrane and boundary conditions:

$$\frac{\mathrm{d}^2\Psi_i}{\mathrm{d}x^2} - \nu_i \frac{\Phi^2}{\alpha_i \gamma_i}\rho = 0, \quad i = \mathrm{A, B, C, D} \tag{1}$$

$$\rho = (\gamma_\mathrm{A}\Psi_\mathrm{A})^a(\gamma_\mathrm{B}\Psi_\mathrm{B})^b - (\gamma_\mathrm{C}\Psi_\mathrm{C})^c(\gamma_\mathrm{D}\Psi_\mathrm{D})^d \frac{C_\mathrm{ref}^{\Delta n}}{K_\mathrm{e}} \tag{2}$$

$$x = 0, \quad \Psi_i = \Psi_i^\mathrm{R} \tag{3}$$

$$x = 1, \quad \Psi_i = \Psi_i^\mathrm{P} \tag{4}$$

Partial and total mass balances in the retentate chamber:

$$\Psi_i^\mathrm{F} - \zeta^\mathrm{R}\Psi_i^\mathrm{R} + \Gamma\, \alpha_i\gamma_i \left.\frac{\mathrm{d}\Psi_i}{\mathrm{d}x}\right|_{x=0} = 0, \quad i = \mathrm{A, B, C, D} \tag{5}$$

$$1 - \zeta^\mathrm{R}\Psi^\mathrm{R} + \Gamma \sum_i \alpha_i\gamma_i \left.\frac{\mathrm{d}\Psi_i}{\mathrm{d}x}\right|_{x=0} = 0, \quad i = \mathrm{A, B, C, D} \tag{6}$$

Partial and total mass balances in the permeate chamber:

$$\zeta^\mathrm{P}\Psi_i^\mathrm{P} + \Gamma\, \alpha_i\gamma_i \left.\frac{\mathrm{d}\Psi_i}{\mathrm{d}x}\right|_{x=1} = 0, \quad i = \mathrm{A, B, C, D} \tag{7}$$

$$\zeta^\mathrm{P}\Psi^\mathrm{P} + \Gamma \sum_i \alpha_i\gamma_i \left.\frac{\mathrm{d}\Psi_i}{\mathrm{d}x}\right|_{x=1} = 0, \quad i = \mathrm{A, B, C, D} \tag{8}$$

and

$$\Psi^\mathrm{R} = \frac{P^\mathrm{R}}{P_\mathrm{ref}}, \quad \Psi^\mathrm{P} = \frac{P^\mathrm{P}}{P_\mathrm{ref}}, \quad \Psi_i = \frac{p_i}{P_\mathrm{ref}}, \quad \Psi_i^\mathrm{F} = \frac{p_i^\mathrm{F}}{P_\mathrm{ref}},$$

$$\Psi_i^\mathrm{P} = \frac{p_i^\mathrm{P}}{P_\mathrm{ref}}, \quad \Psi_i^\mathrm{R} = \frac{p_i^\mathrm{R}}{P_\mathrm{ref}}, \quad \zeta^\mathrm{R} = \frac{Q^\mathrm{R}}{Q_\mathrm{ref}}, \quad \zeta^\mathrm{P} = \frac{Q^\mathrm{P}}{Q_\mathrm{ref}},$$

$$x = \frac{z}{\delta}, \quad \alpha_i = \frac{D_i}{D_\mathrm{ref}}, \quad \gamma_i = \frac{H_i}{H_\mathrm{ref}}, \quad \beta = a + b$$

$$C_\mathrm{ref} = P_\mathrm{ref}H_\mathrm{ref}, \quad \Gamma = \frac{SD_\mathrm{ref}H_\mathrm{ref}\Re T}{\delta Q_\mathrm{ref}}, \quad \Phi = \delta\left(\frac{k_\mathrm{d}C_\mathrm{ref}^{\beta-1}}{D_\mathrm{ref}}\right)^{1/2}$$

The subscripts i and ref refers to the ith and *reference* components and the superscripts F, R and P refer to the feed, retentate and permeate flows, respectively. ψ is the dimensionless pressure, α the dimensionless diffusion coefficient, γ the dimensionless sorption coefficient, ζ the dimensionless total volumetric flow rate and ρ the dimensionless local reaction rate. Φ is the Thiele modulus (a ratio between the characteristic intramembrane diffusion time and the characteristic reaction time) and Γ the dimensionless contact time (a ratio between the total feed flow and the total intramembrane flow). The other symbols are referred in nomenclature. Retentate gas feed conditions are considered as reference for P_ref and Q_ref. Component A is considered as reference for D_ref and H_ref.

The CPDMR conversion, X_A, is calculated by the equation:

$$X_\mathrm{A} = 1 - \frac{\zeta^\mathrm{R}\psi_\mathrm{A}^\mathrm{R} + \zeta^\mathrm{P}\psi_\mathrm{A}^\mathrm{P}}{\zeta^\mathrm{F}\psi_\mathrm{A}^\mathrm{F}} \tag{9}$$

The relative conversion, χ_A, defined as the ratio between the conversion of reactant A, X_A, and the thermodynamic equilibrium conversion based on feed conditions, X_A^e, is used to evaluate the membrane reactor performance.

The reaction coefficient, a measure of how far from equilibrium the reactive system is, is defined as

$$\theta=\frac{(\gamma_{\mathrm{C}}\Psi_{\mathrm{C}})^{c}(\gamma_{\mathrm{D}}\Psi_{\mathrm{D}})^{d}}{(\gamma_{\mathrm{A}}\Psi_{\mathrm{A}})^{a}(\gamma_{\mathrm{B}}\Psi_{\mathrm{B}})^{b}}C_{\mathrm{ref}}^{\Delta n} \tag{10}$$

3. Solution method

The set of equations that governs the CPDMR were solved as follows [42]: a time derivative term was added to the right-hand side of Eqs. (1) and (5)–(8). Eq. (1) was further transformed into a set of ordinary differential equations using orthogonal collocation in finite elements [49] and the resulting time dependent equations were solved using LSODA [50]. The steady-state solution is obtained when a step time increase does not make any further change in the dependent variables, within a pre-defined error.

4. Results and discussion

In this study, we performed several simulations in order to understand how the relative conversion depends on the contact time (Γ) and Thiele modulus (Φ) for different dimensionless diffusion (α) and sorption (γ) coefficients of the reaction products. We consider three different categories of reactions, according to the total net change of the moles number: $\Delta n=0$, $\Delta n<0$ and $\Delta n>0$. The hypothetical reaction considered for all cases is $a\mathrm{A}+b\mathrm{B}\Leftrightarrow c\mathrm{C}+d\mathrm{D}$. In the following discussion, the base case is always taken for dimensionless diffusion and sorption coefficients equal to unity, for all reactants and products. Then some combinations of dimensionless diffusion and sorption coefficients of the reaction product D are studied, so that the permeability becomes smaller or larger than 1. We should remember that the membrane's permeability towards a species depends on the product of its diffusion and sorption coefficients: $L_i=D_iH_i$, or in dimensionless form, $\lambda_i=\alpha_i\gamma_i$, where $\lambda_i=L_i/L_{\mathrm{ref}}$. The fed gas composition ratio (only reactants) was chosen to be at stoichiometric concentration. For a given K_{e} value, this is the ratio composition that gives the highest relative conversion. The value of K_{e} considered for each case is such that the corresponding thermodynamic conversion based on feed conditions, $X_{\mathrm{A}}^{\mathrm{e}}$, is 20%. Finally, $T=300\,\mathrm{K}$, $P_{\mathrm{ref}}=100\,\mathrm{kPa}$, $\Psi^{\mathrm{P}}=0.01$ and $C_{\mathrm{ref}}=100\,\mathrm{mol/m^3}$.

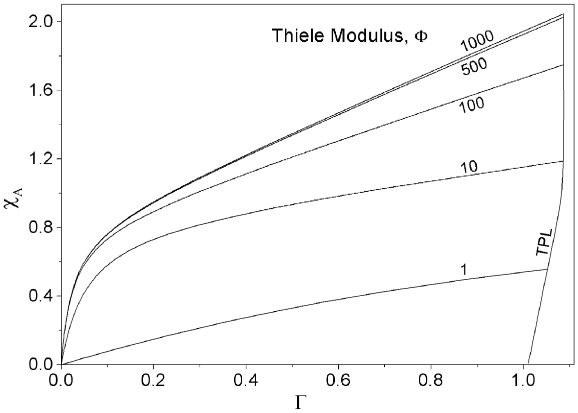

Fig. 2. Relative conversion (χ_{A}) as a function of the contact time (Γ) for various Thiele modulus values (Φ) and for $\Delta n>0$ ($\alpha_i=\gamma_i=1$, $\nu_{i\neq\mathrm{D}}=1$, $\nu_{\mathrm{D}}=2$, $\Psi_{\mathrm{A}}^{\mathrm{F}}=0.5$, $\Psi_{\mathrm{B}}^{\mathrm{F}}=0.5$ and $K_{\mathrm{e}}=1.002\,\mathrm{mol/m^3}$).

4.1. Base case — the permeability is the same for all reactants and products ($\alpha_i=1$; $\gamma_i=1$)

In a previous study [42] it has been shown that for $\alpha_i=1$, $\gamma_i=1$ and $\Delta n=0$ the maximum reached conversion in the CPDMR is equal to the one of thermodynamic equilibrium. For reactions where $\Delta n>0$ (Fig. 2) or $\Delta n<0$ (Fig. 3), however, the maximum

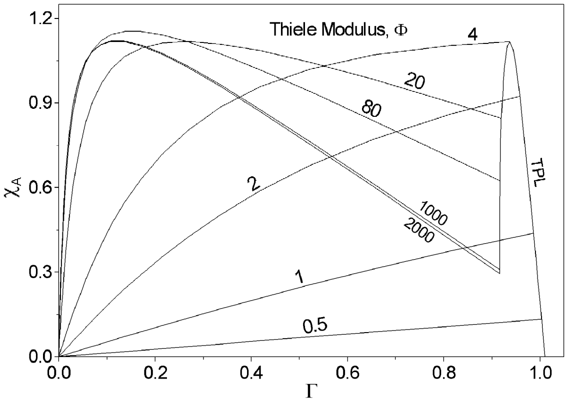

Fig. 3. Relative conversion (χ_{A}) as a function of the contact time (Γ) for various Thiele modulus values (Φ) and for $\Delta n<0$ ($\alpha_i=\gamma_i=1$, $\nu_{i\neq\mathrm{B}}=1$, $\nu_{\mathrm{B}}=2$, $\Psi_{\mathrm{A}}^{\mathrm{F}}=0.333$, $\Psi_{\mathrm{B}}^{\mathrm{F}}=0.667$ and $K_{\mathrm{e}}=0.00146\,\mathrm{m^3/mol}$).

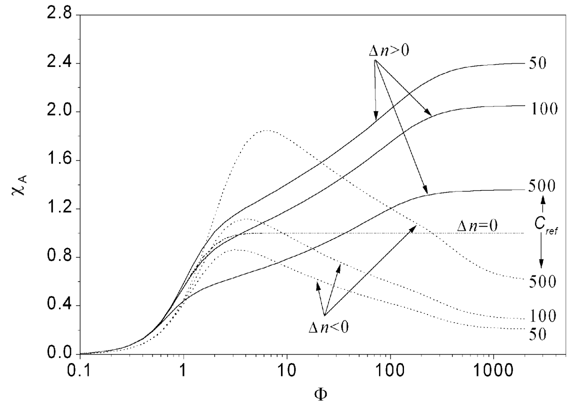

Fig. 4. Relative conversion (χ_A) in the TPC as a function of the Thiele modulus values (Φ) for different C_{ref} values and reaction categories: $\Delta n < 0$ ($\nu_{i\neq B} = 1$, $\nu_B = 2$, $\Psi_A^F = 0.333$, $\Psi_B^F = 0.667$ and $K_e = 0.00146\,m^3/mol$); $\Delta n = 0$ ($\nu_i = 1$, $\Psi_A^F = 0.5$, $\Psi_B^F = 0.5$ and $K_e = 0.0625\,m^3/mol$) and $\Delta n > 0$ ($\nu_{i\neq D} = 1$, $\nu_D = 2$, $\Psi_A^F = 0.5$, $\Psi_B^F = 0.5$ and $K_e = 1.002\,mol/m^3$). Other variables are: $\alpha_i = 1$, $\gamma_i = 1$.

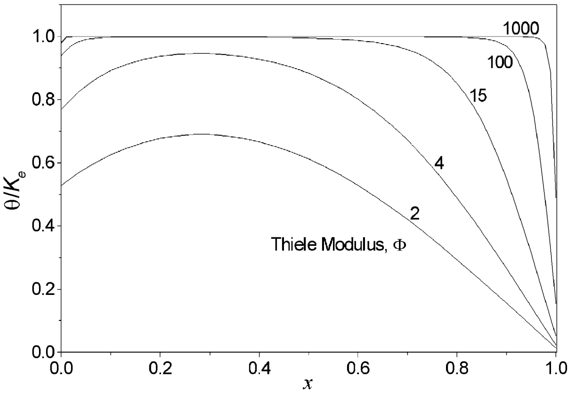

Fig. 5. Relative reaction coefficient (θ/K_e) in TPC as a function of the spatial coordinate of the membrane (x) for various Thiele modulus values (Φ) and for $\Delta n > 0$ (same parameter values as in Fig. 2).

conversion attained in the CPDMR can be larger than the thermodynamic equilibrium value, depending on the average concentration inside the membrane (Fig. 4).

Fig. 2 shows the relative conversion as a function of the contact time for various Thiele moduli and for $\Delta n > 0\,(a = b = c = 1, d = 2)$. In this case, the CPDMR conversion enhancement, when compared with the thermodynamic equilibrium value, is only due to the pressure gradient imposed across the membrane — *total concentration effect* (according to the Le Chatelier principle). This conversion enhancement is favoured by a low average concentration of reagents inside the membrane (Fig. 4). The relative conversion increases continuously with Γ until the total permeation condition, TPC (i.e., no flow out from the retentate chamber [42]), where the reacting species have the highest possible contact time with the catalyst in the membrane (Fig. 2). The relative conversion increases also continuously with Φ (Fig. 2) until reaction is in local equilibrium throughout the catalytic membrane (Fig. 5). This happens because the shift in the chemical equilibrium, induced by the total concentration effect, is favoured by a high reaction rate. It is worth noting that the increase of the contact time in the TPC as a function of the Thiele modulus (total permeation line, TPL, in Fig. 2) does not follow the increase of the conversion, for the same operation conditions. This happens because the composition of the retentate side reaches a nearly constant value at relatively low Thiele modulus, when the local equilibrium front is very close to the membrane surface on the retentate side (Fig. 5). Further increase of the conversion is only due to the displacement of the local equilibrium front to the membrane surface on the permeate side (Fig. 5).

The relative conversion as a function of the contact time for various Thiele moduli and for $\Delta n < 0\,(a = c = d = 1, b = 2)$ is given in Fig. 3. For this case, the pressure gradient imposed on the membrane is unfavourable, because it favours the backward reaction (in the fraction of the membrane thickness where $\theta > K_e$, Fig. 6). This effect was named *backward reaction effect*. In this case, the CPDMR conversion is favoured by a high average concentration inside the membrane (Fig. 4). The competition between the reaction rate and the diffusional transport defines two different operation zones, with the boundary set for $\Phi = 4$ (Fig. 3). For the chemical regime operation ($\Phi < 4$), the reaction rate is lower than the diffusional transport and the maximum relative conversion is attained in the TPC, when the contact time of the reactants with the catalyst is maximum. The backward reaction that occurs inside the membrane is offset by the diffusion transport. For diffusional regime operation ($\Phi > 4$), there is a turning point in the curves.

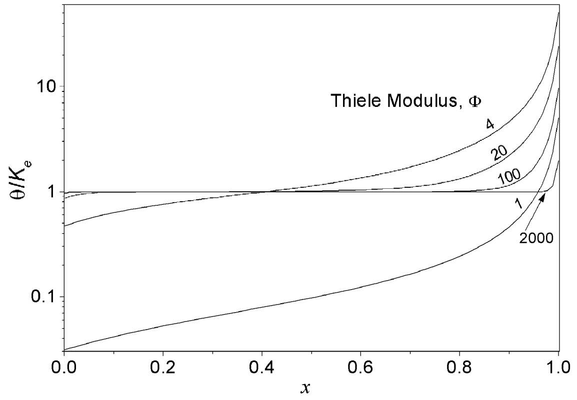

Fig. 6. Relative reaction coefficient (θ/K_e) in TPC as a function of the spatial coordinate of the membrane (x) for various Thiele modulus values (Φ) and for $\Delta n < 0$ (same parameter values as in Fig. 3).

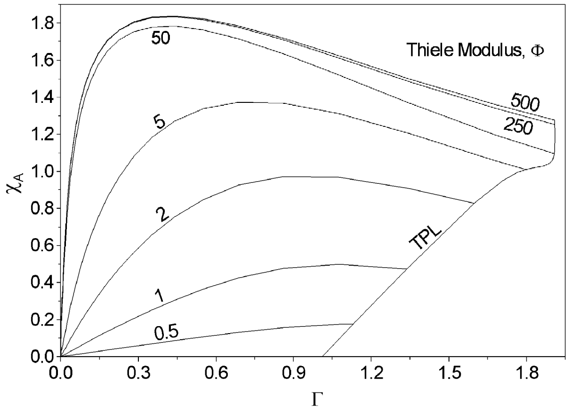

Fig. 7. Relative conversion (χ_A) as a function of the contact time (Γ) for various Thiele modulus values (Φ) and for $\Delta n = 0$ ($\alpha_i = 1$, $\gamma_{i\neq D} = 1$, $\gamma_D = 0.1$, $\nu_i = 1$, $\Psi_A^F = 0.5$, $\Psi_B^F = 0.5$ and $K_e = 0.0625\,\mathrm{m^3/mol}$).

The contact time value for the maximum relative conversion (Γ_{MC}) is lower than the contact time value in the TPC and it decreases with Φ. For $\Gamma < \Gamma_{MC}$, the ratio between the flux of the reaction products in the retentate stream and across the membrane is high enough to offset the backward reaction effect and the conversion increases with Γ, again due to an increase on the contact time of the reactants. For $\Gamma > \Gamma_{MC}$, the diffusion transport of the reaction products across the membrane is high enough and the backward reaction effect leads to a decrease in the conversion as a function of Γ. Γ_{MC} decreases with an increase of Φ due to the shift of the local equilibrium front towards the membrane surface on the retentate side (Fig. 6). The contact time decreases continuously with Thiele modulus in the TPC (Fig. 3), not following the conversion trend for the same operating conditions, as in the previous example ($\Delta n > 0$). In this case, the contact time in TPC reflects the balance of two trends: increasing the conversion leads to a decrease in the total number of moles, resulting in a contact time decrease, and vice versa. On the other hand, increasing the Thiele modulus shifts the local equilibrium front to a membrane axial position closer to the retentate side (Fig. 6), reducing the path that the reactants have to travel until reaching local equilibrium (Fig. 3). This way, the total number of moles inside the membrane diminishes (due to the reaction's stoichiometry) and the contact time decreases.

4.2. Permeability of component D (product) smaller than 1

For $\Delta n = 0$, we showed in a previous study [42] that the permeability of the reactants and products affect the CPDMR conversion in two different ways. Decreasing the permeability by lowering the diffusion coefficients of products is unfavourable, since the CPDMR conversion becomes smaller than the equilibrium one. In the other way, decreasing the permeability by lowering the sorption coefficients of the reaction products is favourable, as the CPDMR conversion could become higher than the equilibrium one. Fig. 7 illustrates these conclusions. For $\Delta n \neq 0$ (Figs. 8 and 9), the CPDMR conversion depends also on the sorption and diffusion coefficients of reaction product (*selective separation effect*) as well as on Δn and C_{ref}. Anyway, lower products sorption coefficients are far more favourable than lower diffusion coefficients, independently of the other parameters.

Fig. 8 shows the relative conversion as a function of the contact time for various Thiele moduli with $\Delta n > 0\,(a = b = c = 1, d = 2)$ and $\gamma_D = 0.1$. As we can see in this figure, the CPDMR conversion can attain values well above the thermodynamic equilibrium. Comparing these results with that of Fig. 7 (where only the selective separation effect is present) and Fig. 2 (where only the total concentration effect is present) we notice that for high Φ values, the

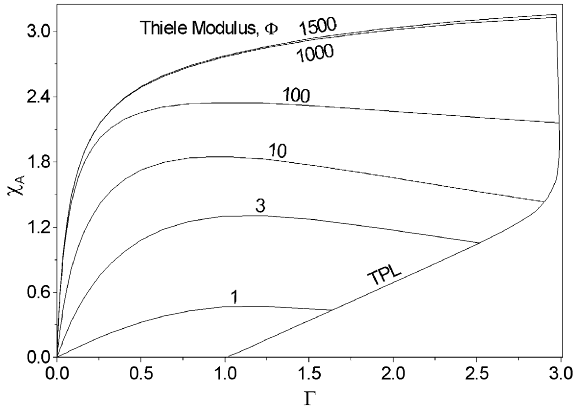

Fig. 8. Relative conversion (χ_A) as a function of the contact time (Γ) for various Thiele modulus values (Φ) and for $\Delta n > 0$ ($\alpha_i = 1$, $\gamma_{i\neq D} = 1$, $\gamma_D = 0.1$, $\nu_{i\neq D} = 1$, $\nu_D = 2$, $\Psi_A^F = 0.5$, $\Psi_B^F = 0.5$ and $K_e = 1.002\,\mathrm{mol/m^3}$).

conversion increases continuously until the TPC. This means that the total concentration effect overcomes the selective separation one. Conversely, for medium Φ values the relative conversion curves show a turning point. In this case, the selective separation effect overcomes the total concentration effect. For these Thiele modulus values, the relative conversion decreases with the contact time after the turning point, because, due to the reactants higher permeability, a fraction of these crosses the membrane without reacting.

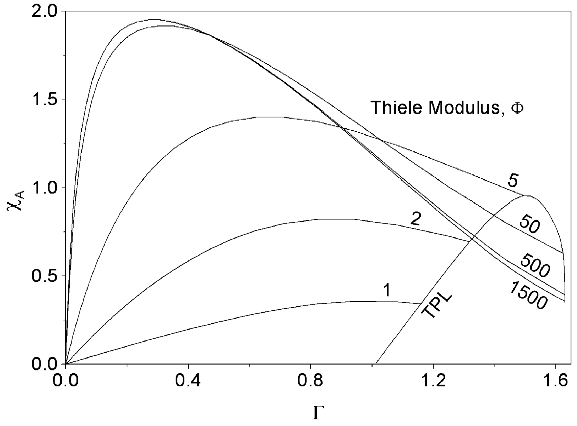

Fig. 9. Relative conversion (χ_A) as a function of the contact time (Γ) for various Thiele modulus values (Φ) and for $\Delta n < 0$ ($\alpha_i = 1$, $\gamma_{i\neq D} = 1$, $\gamma_D = 0.1$, $\nu_{i\neq B} = 1$, $\nu_B = 2$, $\Psi_A^F = 0.333$, $\Psi_B^F = 0.667$ and $K_e = 0.00146\,\mathrm{m^3/mol}$).

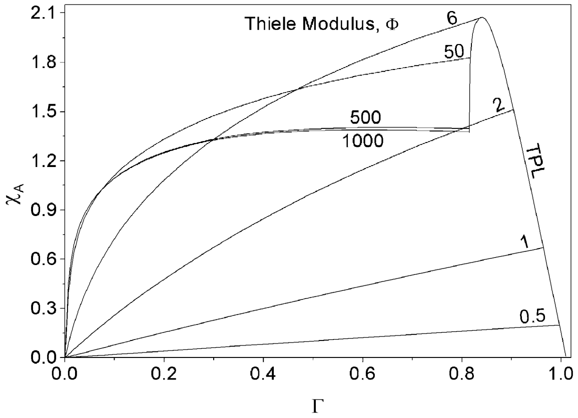

Fig. 10. Relative conversion (χ_A) as a function of the contact time (Γ) for various Thiele modulus values (Φ) and for $\Delta n = 0$ ($\alpha_{i\neq D} = 1$, $\gamma_i = 1$, $\alpha_D = 10$, $\nu_i = 1$, $\Psi_A^F = 0.5$, $\Psi_B^F = 0.5$ and $K_e = 0.0625\,\mathrm{m^3/mol}$).

The relative conversion as a function of the contact time for various Thiele moduli with $\Delta n < 0\,(a = c = d = 1, b = 2)$ and $\gamma_D = 0.1$ is presented in Fig. 9. These results show a contribution of the total concentration effect (see Fig. 3) and the selective separation effect (see Fig. 7) on the CPDMR conversion and on the contact time in TPC. For low Φ values, the selective separation effect is dominant, while for medium/high Φ values the total concentration effect is the most important one.

4.3. Permeability of component D (product) greater than 1

For $\Delta n = 0$, increasing the permeability by increasing the diffusivity coefficients is far more favourable for the CPDMR conversion than increasing the sorption coefficient [42]. Fig. 10 illustrates these conclusions. For $\Delta n \neq 0$ (Figs. 11 and 12), the CPDMR conversion depends also on the sorption and diffusion coefficients of reaction product (selective separation effect) as well as on Δn and C_{ref}.

In Fig. 11 the relative conversion as a function of the contact time is presented for various Thiele moduli, with $\Delta n > 0\,(a = b = c = 1, d = 2)$ and $\alpha_D = 10$. These results show that the contact time in TPC is controlled essentially by the selective separation effect while the CPDMR conversion shows a

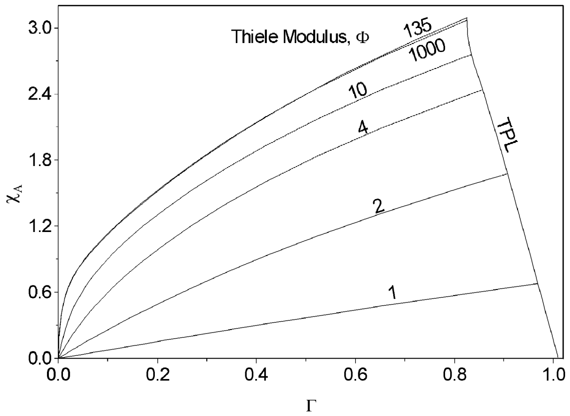

Fig. 11. Relative conversion (χ_A) as a function of the contact time (Γ) for various Thiele modulus values (Φ) and for $\Delta n > 0$ ($\alpha_{i \neq D} = 1$, $\gamma_i = 1$, $\alpha_D = 10$, $\nu_{i \neq D} = 1$, $\nu_D = 2$, $\Psi_A^F = 0.5$, $\Psi_B^F = 0.5$ and $K_e = 1.002\,\text{mol/m}^3$).

clear overlapping of the total concentration effect. The selective separation effect in the CPDMR conversion should only be important for high Thiele modulus values ($\Phi > 135$, in this case). However, for high values of the Thiele modulus the reaction attains the local equilibrium very soon in the membrane and the conversion is no longer affected by the separation, staying nearly constant as a function of the Thiele modulus.

The relative conversion as a function of the contact time for various Thiele moduli, with $\Delta n < 0$ ($a = c = d = 1, b = 2$) and $\alpha_D = 10$ is shown in Fig. 12. The resulting curves share some pattern similarities with Figs. 3 and 10, where the backward reaction effect is present. The total concentration effect is dominant for high Thiele moduli.

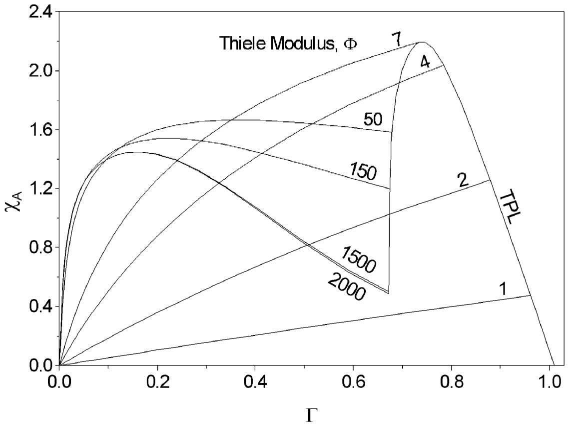

Fig. 12. Relative conversion (χ_A) as a function of the contact time (Γ) for various Thiele modulus values (Φ) and for $\Delta n < 0$ ($\alpha_{i \neq D} = 1$, $\gamma_i = 1$, $\alpha_D = 10$, $\nu_{i \neq B} = 1$, $\nu_B = 2$, $\Psi_A^F = 0.333$, $\Psi_B^F = 0.667$ and $K_e = 0.00146\,\text{m}^3/\text{mol}$).

5. Conclusions

An isothermal polymeric catalytic non-porous membrane reactor, with a perfectly mixed flow pattern in the retentate and permeate chambers, was simulated for the equilibrium gas-phase reaction $a\text{A} + b\text{B} \Leftrightarrow c\text{C} + d\text{D}$ and for three different cases: $\Delta n > 0$, $\Delta n = 0$ and $\Delta n < 0$.

The results show that the CPDMR could be very attractive for conducting gas-phase equilibrium reactions, especially when $\Delta n > 0$. For this reaction category, conversion enhancement is favoured by high Thiele modulus and contact time values. A low total average concentration inside the membrane favours the CPDMR conversion.

When $\Delta n < 0$, it is still possible to obtain relative conversion enhancements. However, due to the undesirable equilibrium shift induced by the pressure gradient imposed across the membrane (backward reaction effect), possible enhancements are more modest. For this reaction category, conversion enhancement is favoured by medium Thiele modulus and high contact time values. A high average total concentration inside the membrane favours the CPDMR conversion.

For the three reaction categories studied, the conversion enhancement is favoured by higher diffusion and lower sorption coefficients of the products. It is, however, preferable to have higher diffusion coefficients, because the contact time in TPC is then lower, leading to smaller reactors size.

Since the performance of a non-porous membrane reactor depends in a different way on both the sorption and diffusion coefficients, a study of such reactors cannot be based exclusively on the permeabilities of reactants and products.

Acknowledgements

José M. Sousa acknowledges a grant from FCT to attend to the ICCMR 2000 congress and Paulo Cruz acknowledges a Ph.D. grant from PRAXIS XXI program, BD/21483/99. The authors also acknowledge Prof. Fernão D. Magalhães for his careful revision of the manuscript.

References

[1] W.J. Koros, R.T. Chern, Separation of gaseous mixtures using polymer membranes, in: R.W. Rousseau (Ed.), Handbook of Separation Process Technology, Wiley, New York, 1987, pp. 862–953.

[2] I.F.J. Vankelecom, K.A.L. Vercruysse, P.E. Neys, D.W.A. Tas, K.B.M. Janssen, P.-P. Knops-Gerrits, P.A. Jacobs, Novel catalytic membranes for selective reactions, Topics Catal. 5 (1998) 125.

[3] J. Sanchez, T.T. Tsotsis, Current developments and future research in catalytic membrane reactors, in: A.J. Burggraaf, L. Cot (Eds.), Fundamentals of Inorganic Science and Technology, Elsevier, Amsterdam, 1996, pp. 529–568.

[4] S. Tennison, Current hurdles in the commercial development of inorganic membrane reactor, in: Proceedings of the Fourth International Conference on Catalysis in Membrane Reactors, Zaragoza, Spain, July 3–5, 2000, pp. 13–17.

[5] K.K. Sirkar, P.V. Shanbhag, A.S. Kovvali, Membrane in a reactor: a functional perspective, Ind. Eng. Chem. Res. 38 (1999) 3715.

[6] I.F.J. Vankelecom, P.A. Jacobs, Dense organic catalytic membranes for fine chemical synthesis, Catal. Today 56 (2000) 147.

[7] M. Grayson, D. Eckroth (Eds.), Kirk-Othmer Encyclopedia of Chemical Technology, Vol. 21, 3rd Edition, Wiley, New York, 1983, pp. 770–801.

[8] J.F. Ciebien, R.E. Cohen, A. Duran, Catalytic properties of palladium nanoclusters synthesized within diblock copolymer films: hydrogenation of ethylene and propylene, Supramol. Sci. 5 (1998) 31.

[9] J. Shu, B.P.A. Grandjean, A. van Neste, S. Kaliaguine, Catalytic palladium-based membrane reactors — a review, Can. J. Chem. Eng. 69 (1991) 1036.

[10] V.M. Gryaznov, A.P. Maganjuk, S.F. Gizhevskii, New membrane reactors for liquid phase hydrogenation, in: Proceedings of the Ravello Conference on New Frontiers for Catalytic Membrane Reactors and other Membrane Systems, Ravello, Italy, May 23–27, 1999, pp. 45–48.

[11] V.M. Gryaznov, M.M. Ermilova, N.V. Orekhova, Membrane–catalyst systems for selectivity improvement, in: Proceedings of the Fourth International Conference on Catalysis in Membrane Reactors, Zaragoza, Spain, July 3–5, 2000, pp. 31–32.

[12] T.M. Raybold, M.C. Huff, Oxidation of isobutane over supported noble metal catalysts in a palladium membrane reactor, Catal. Today 56 (2000) 35.

[13] O. Schramm, A. Seidel-Morgenstern, Comparing porous and dense membranes for the application in membrane reactors, Chem. Eng. Sci. 54 (1999) 1447.

[14] H. Weyten, K. Keizer, A. Kinoo, J. Luyten, R. Leysen, Dehydrogenation of propane using a packed-bed catalytic membrane reactor, AIChE J. 43 (1997) 1819.

[15] J. Szegner, K.L. Yeung, A. Varma, Effect of catalyst distribution in a membrane reactor: experiments and model, AIChE J. 43 (1997) 2059.

[16] Y.V. Gokhale, R.D. Noble, J.L. Falconer, Effects of reactant loss and membrane selectivity on a dehydrogenation in a membrane-enclosed catalytic reactor, J. Memb. Sci. 103 (1995) 235.

[17] E. Gobina, K. Hou, R. Hughes, Ethane dehydrogenation in a catalytic membrane reactor coupled with a reactive sweep gas, Chem. Eng. Sci. 50 (1995) 2311.

[18] H. Weyten, J. Luyten, K. Keizer, L. Willems, R. Leysen, Membrane performance: the key issues for dehydrogenation reactions in a catalytic membrane reactor, Catal. Today 56 (2000) 3.

[19] R. Dittmeyer, V. Höllein, P. Quicker, G. Emig, G. Hausinger, F. Schmidt, Factors controlling the performance of catalytic dehydrogenation of ethylbenzene in palladium composite membrane reactor, Chem. Eng. Sci. 54 (1999) 1431.

[20] N. Itoh, K. Haraya, A carbon membrane reactor, Catal. Today 56 (2000) 103.

[21] M.E. Rezac, B. Bayer, E.T. Sorensen, N. Karangu, H.W. Beckham, Cross-linkable polyimides for improved membrane stability, in: Proceedings of the Progress in Membrane Science and Technology, Euromembrane'97, University of Twente, the Netherlands, June 23–27, 1997, pp. 11–13.

[22] G. Langhendries, G.V. Baron, I.F.J. Vankelecom, R.F. Parton, P.A. Jacobs, Selective hydrocarbon oxidation using a liquid-phase catalytic membrane reactor, Catal. Today 56 (2000) 131.

[23] H.L. Frisch, S. Maaref, H. Deng-Nemer, Low-temperature dehydrogenation reaction–separation membrane using zeolite 13X polyethylacrylate, J. Memb. Sci. 154 (1999) 33.

[24] I.F.J. Vankelecom, N.M.F. Moens, K.A.L. Vercruysse, R.F. Parton, P.A. Jacobs, PDMS occluded Ti-MCM-41 as an improved olefin epoxidation catalyst, in: H.U. Blaser, A. Baiker, R. Prins (Eds.), Heterogeneous Catalysis and Fine Chemicals IV, Elsevier, Amsterdam, 1997, pp. 437–444.

[25] P.E.F. Neys, A. Severeyns, I.F.J. Vankelecom, E. Ceulemans, W. Dehaen, P.A. Jacobs, Manganese porphyrins incorporated in PDMS: selective catalysts for the epoxidation of deactivated alkenes, J. Mol. Catal. 144 (1999) 373.

[26] R.A. Sheldon, Selective catalytic synthesis of fine chemicals: opportunities and trends, J. Mol. Catal. A 107 (1996) 75.

[27] S. Kaliaguine, C. Bouchard, S.Q. Wu, J. Shu, Use of catalytic membranes as interphase contactors for multiphase reactions, Canadian Patent 2,206,626 (1998).

[28] S. Wu, J.-E. Gallot, M. Bousmina, C. Bouchard, S. Kaliaguine, Zeolite containing catalytic membranes as interphase contactors, Catal. Today 56 (2000) 113.

[29] C. Liu, Y. Xu, S. Liao, D. Yu, Y. Zhao, Y. Fan, Selective hydrogenation of propadiene and propyne in propene with catalytic polymeric hollow-fiber reactor, J. Memb. Sci. 137 (1997) 139.

[30] D. Fritsch, K.V. Peinemann, Catalysis with homogeneous membranes loaded with nanoscale metallic clusters and their preparation, Catal. Today 25 (1995) 277.

[31] D. Fritsch, K.-V. Peinemann, Novel highly permselective 6*F*-poly(amide–imide)s as membrane host for nano-sized catalysts, J. Memb. Sci. 99 (1995) 29.

[32] H. Gao, S. Liao, Y. Xu, R. Liu, J. Liu, D. Li, Selective hydrogenation of cyclopentadiene in a catalytic cellulose acetate hollow fiber reactor, Catal. Lett. 27 (1994) 297.

[33] H. Gao, Y. Xu, S. Liao, R. Liu, J. Liu, D. Li, D. Yu, Y. Zhao, Y. Fan, Catalytic polymeric hollow-fiber reactors for selective hydrogenation of conjugated dienes, J. Memb. Sci. 106 (1995) 213.

[34] J.F. Ciebien, R.E. Cohen, A. Duran, Membrane catalysts for partial hydrogenation of 1,3-butadiene: catalytic properties of palladium nanoclusters synthesized within diblock copolymer films, Mater. Sci. Eng. C 7 (1999) 45.

[35] J. Theis, D. Fritsch, F. Keil, ESF network catalytic membrane reactors, in: Proceedings of the Applications and Future Possibilities of Catalytic Membrane Reactors, Turnhout, Belgium, October 16–17, 1997, pp. 35–40.

[36] J.S. Choi, I.K. Song, W.Y. Lee, Performance of shell and tube-type membrane reactors equipped with heteropolyacid–polymer composite catalytic membranes, in: Proceedings of the Fourth International Conference on Catalysis in Membrane Reactors, Zaragoza, Spain, July 3–5, 2000, pp. 181–182.

[37] A.M. Champagnie, T.T. Tsotsis, R.G. Minet, E. Wagner, The study of ethane dehydrogenation in a catalytic membrane reactor, J. Catal. 134 (1992) 713.

[38] G. Saracco, J.W. Veldsink, G.F. Versteeg, W.P.M. van Swaaij, Catalytic combustion of propane in a membrane reactor with separate feed of reactants. II. Operation in presence of trans-membrane pressure gradients, Chem. Eng. Sci. 50 (1995) 2833.

[39] J.S. Choi, I.K. Song, W.Y. Lee, Simulation and experimental study on the polymer membrane reactors for the vapor-phase MTBE decomposition, Catal. Today 56 (2000) 275.

[40] Y.-M. Sun, S.-J. Khang, A catalytic membrane reactor: its performance in comparison with other types of reactors, Ind. Eng. Chem. Res. 29 (1990) 232.

[41] C. Hermann, P. Quicker, R. Dittmeyer, Mathematical simulation of catalytic dehydrogenation of ethylbenzene to styrene in a composite palladium membrane reactor, J. Memb. Sci. 136 (1997) 161.

[42] J.M. Sousa, P. Cruz, A. Mendes, Modelling a catalytic polymeric non-porous membrane reactor, J. Memb. Sci. 181 (2001) 241.

[43] K. Mohan, R. Govind, Analysis of equilibrium shift in isothermal reactors with a permselective wall, AIChE J. 34 (1988) 1493.

[44] K.L. Yeung, R. Aravind, R.J.X. Zawada, J. Szegner, G. Cao, A. Varma, Non-uniform catalyst distribution for inorganic membrane reactors: theoretical considerations and preparation techniques, Chem. Eng. Sci. 49 (1995) 4823.

[45] M.K. Koukou, G. Chaloulou, N. Papayannakos, N.C. Markatos, Mathematical modelling of the performance of non-isothermal membrane reactors, Int. J. Heat Mass Transfer 40 (1997) 2407.

[46] M.P. Harold, C. Lee, Intermediate product yield enhancement with a catalytic inorganic membrane. II. Nonisothermal and integral operation in a back-mixed reactor, Chem. Eng. Sci. 52 (1997) 1923.

[47] R.P. Omorjan, G.M. Ciric, M.N. Tekic, R.N. Paunovic, Applicability of two-membrane reactors for reversible gas phase reaction. Effects of flow patterns and inerts, J. Memb. Sci. 128 (1997) 213.

[48] R.P. Omorjan, R.N. Paunovic, M.N. Tekic, Applicability of a double-membrane reactor for thermal decomposition of water: a computer analysis, J. Memb. Sci. 154 (1999) 273.

[49] B.A. Finlayson, Nonlinear Analysis in Chemical Engineering, McGraw-Hill, New York, 1980.

[50] L.R. Petzold, A.C. Hindmarsh, LSODA, Computing and Mathematics Research Division, Lawrence Livermore National Laboratory, 1997.